

Jeffrey R. Key^{1*}, David Santek², Christopher S. Velden², and W. Paul Menzel¹

¹Office of Research and Applications, National Environmental Satellite, Data, and Information Service, NOAA
1225 West Dayton Street, Madison, WI, 53706

²Cooperative Institute for Meteorological Satellite Studies, University of Wisconsin-Madison
1225 West Dayton Street, Madison, WI, 53706

1. INTRODUCTION

In the early 1960s Tetsuya Fujita developed analysis techniques to use cloud pictures from the first TIROS polar orbiting satellite for estimating the velocity of tropospheric winds (Menzel, 2001). Throughout the 1970s and early 1980s cloud motion winds were produced from satellite data using a combination of automated and manual techniques. In 1992, the National Oceanic and Atmospheric Administration (NOAA) began using an automated winds software package that made it possible to produce a full-disk wind set without manual intervention. The carbon dioxide (CO₂) slicing algorithm (Menzel et al., 1983) made it possible to assign accurate cloud heights to the motion vectors. Fully automated cloud-drift wind production from the Geostationary Operational Environmental Satellites (GOES) became operational in 1996, and now wind vectors are routinely used in operational numerical models of the National Centers for Environmental Prediction (NCEP).

Satellite-derived wind fields are most valuable for the oceanic regions where few observations exist and numerical weather prediction model forecasts are less accurate as a result. Like the oceans at lower latitudes, the polar regions also suffer from a lack of observational data. While there are land-based meteorological stations in the Arctic, and a small number of stations around the coast of Antarctica, there are no routine observations of winds over the Arctic Ocean and most of the Antarctic continent. Unfortunately, geostationary satellites are of little use at high latitudes due to the large view angles and poor spatial resolution, resulting in large uncertainties in the derived wind vectors.

Can polar-orbiting satellites be used to obtain wind information at high latitudes? Difficulties arise from the irregular temporal sampling and viewing geometry, but the idea has been explored before with promising results. The Advanced Very High Resolution Radiometer (AVHRR) was used by Herman (1993) to estimate cloud-drift winds for a few Arctic scenes. When compared to rawinsonde winds, the AVHRR winds were found to have a root-mean-square error of 6 m s⁻¹. Herman and Nagle (1994) compared cloud-drift winds from the AVHRR using two different methods of obtaining

cloud height to gradient winds computed with the HIRS sounder. The AVHRR cloud-drift winds that incorporated the CO₂ slicing method (using HIRS channels) were found to be comparable to the HIRS gradient winds, with root-mean-square errors less than 5 m s⁻¹. Turner and Warren (1989) obtained useful cloud track wind information from AVHRR Global Area Coverage (GAC) data in the Weddell Sea, Antarctica.

In this paper we discuss a new effort to obtain estimates of high-latitude tropospheric winds using the MODerate Resolution Imaging Spectroradiometer (MODIS) on-board the National Aeronautics and Space Administration's (NASA) polar orbiting Terra satellite. Sampling issues are discussed, and results from a case study are presented.

2. TEMPORAL SAMPLING

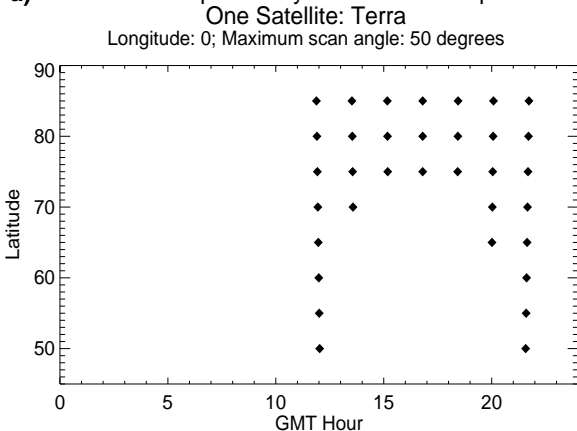
Statistical analyses of visible, infrared, and water vapor wind data sets from geostationary satellites versus rawinsonde verification data have shown that the optimal processing intervals are 5 minutes for visible imagery of 1 km resolution, 10 minutes for infrared imagery of 4 km resolution, and 30 minutes for water vapor imagery of 8 km resolution. How often can we obtain wind vectors from a polar-orbiting satellite? Not surprisingly, the answer depends on the latitude and the number of satellites. Figure 1a shows the frequency of time differences between successive overpasses at a given latitude-longitude point on a single day with only one satellite. At 60° latitude there are two overpasses separated by about 10 hours. Obviously, no useful wind information can be obtained at this latitude with only a single satellite. At 80° there are many views separated by 100 minutes (the orbital period), but there is still a 13 hour gap each day. Even with large gaps at a single location, however, wind vectors can be obtained during part of every day for the entire Arctic and Antarctic regions.

Figure 1b shows the coverage with multiple satellites: the current NOAA-15, NOAA-16, Terra, and Chinese FY-1C satellites and NASA's future Aqua platform. Orbital characteristics based on current plans for Aqua were used in the simulation. Temporal gaps of a few hours still exist at the lower latitudes of the polar regions but at the higher latitudes the temporal coverage is very good. Given that geostationary satellites provide wind information equatorward of about 60 degrees latitude, global coverage can be obtained by using polar-orbiting satel-

* Corresponding author address: Jeff Key, NOAA/NESDIS, 1225 West Dayton Street, Madison, WI 53706; e-mail: jkey@ssec.wisc.edu.

lites for the high-latitudes, though two or more will be required to satisfy temporal sampling requirements.

a) Satellite Overpasses by Latitude on 1 Sep 2000



b) Satellite Overpasses by Latitude on 1 Sep 2000

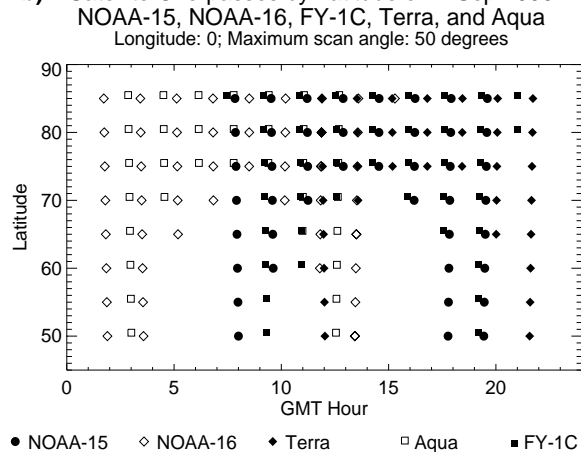


Fig. 1. (a) Time differences between successive overpasses of a single satellite (Terra) as a function of latitude over the course of a day at the Prime Meridian. Only overpasses with view angles less than 50 degrees are considered. (b) Time differences between successive overpasses of five satellites.

3. METHODS

Cloud and water vapor tracking with MODIS data is based on the established procedure used for GOES, which is essentially that described in Merrill (1989), Nieman et al. (1997), and Velden et al. (1997). With MODIS, cloud features are tracked in the infrared window band at 11 μm ; water vapor features are tracked in the 6.7 μm band.

After remapping the orbital data to a polar stereographic projection, potential tracking features are identified. The lowest brightness temperature in the infrared window band (generally indicating cloud) within a target box is isolated and local gradients are computed. The

size of the target area controls the density of derived vectors. Gradients that exceed a specified threshold are classified as targets for tracking. For water vapor target selection, local gradients are computed for the area surrounding every pixel rather than the single pixel with the minimum brightness temperature in a box. Water vapor targets are selected in both cloudy and cloud-free regions.

The tracking method employs a simple search for the minimum of the sum of squared radiance differences between the target and the search boxes in two subsequent images. A model forecast of the upper level wind is used to choose the appropriate search areas. Displacement vectors are derived for each of the two subsequent images. They are then subject to consistency checks to eliminate accelerations that exceed empirically determined tolerances. A final step in the tracking process is an adjustment to the vector speed for a well-documented slow bias in the upper-tropospheric cloud-tracked winds.

Height assignments can be made with any of three methods. The infrared window method assumes that the mean of the coldest values in a sample is the temperature at the cloud top. The temperature is compared to a numerical forecast of the vertical temperature profile to determine the cloud height. This method is reasonably accurate for opaque clouds, but inaccurate for semi-transparent clouds.

The CO₂ slicing method works well for both opaque and semitransparent clouds. Cloudy and clear radiance differences in the CO₂ (13.3 μm) and infrared window bands are ratioed and compared to the theoretical ratio of the same quantities, calculated for a range of cloud pressures. The cloud pressure that gives the best match between the observed and theoretical ratios is chosen (Menzel et al., 1983; Frey et al., 1999).

The H₂O-intercept method of height determination can be used as an additional metric or, in the case of some other polar-orbiting imagers, in the absence of a CO₂ band. This method examines the linear trend between clusters of clear and cloudy pixel values in water vapor-infrared window brightness temperature space, predicated on the fact that radiances from a single cloud deck for two spectral bands vary linearly with cloud amount. The line connecting the clusters is compared to theoretical calculations of the radiances for different cloud pressures. The intersection of the two gives the cloud height (Schmetz et al., 1993).

We are investigating cloud height assignment where the results of the MODIS cloud product algorithm (Menzel and Strabala, 1997) are incorporated into the processing stream. Cloud top pressure is derived from a multi-channel CO₂ slicing technique and the cloud mask.

After wind vectors are determined and heights are assigned, the resulting data set is subject to a postprocessing, quality-control step. The purposes of this step are to determine the tropospheric level that best represents the motion vector being traced, to edit out vectors

that are in obvious error, and to provide end users with vector quality information (Velden et al., 1998).

4. APPLICATION

Figure 2 illustrates the application of the method to MODIS data. The figure shows wind vectors derived from both cloud and water vapor tracking in three consecutive overpasses on 6 September 2000 over the western Arctic Ocean. Portions of the underlying infrared image are devoid of wind vectors because those areas were not observed in subsequent overpasses. The three overpasses were separated by approximately 100 minutes for a total time span of 3.3 hours.

Vector heights, which represent the height of the cloud or water vapor feature that was tracked, are given in three broad categories: low (white), middle (grey), and high (black). Lower tropospheric wind estimates occur within the cyclonic system north of Siberia and also just east of 120 E longitude; mid-level, high velocity winds were measured in and around the frontal structure extending from the lower center portion of the image through the New Siberian Islands and also northeast of Wrangel Island in the bottom left portion of the image. Vectors for upper-level winds, primarily from the water vapor band, occur throughout the field.

5. CONCLUSIONS

This study has demonstrated the feasibility of deriving tropospheric wind information at high latitudes from polar-orbiting satellites. The methodology employed is based on the algorithms currently used with geostationary satellites, modified for use with the polar-orbiting MODIS instrument.

The project presents some unique challenges, including the irregularity of temporal sampling, different viewing geometries from one image to the next, large uncertainties in the model forecast profiles used in height assignment and quality control, and the complexity of surface features, including their motion. These and other issues will be investigated in the future, as part of an extensive processing and validation campaign. Model impact studies are also planned.

Acknowledgments. This work was supported by NOAA contract NA07EC0676.

6. REFERENCES

Frey, R., B. A. Baum, W. P. Menzel, S.A. Ackerman, C.C. Moeller, and J. D. Spinhirne, 1999: A comparison of cloud top heights computed from airborne LIDAR and MAS radiance data using CO₂-slicing. *J. Geophys. Res.*, 104(D20), 24,547-24,555.

- Herman, L.D., 1993: High frequency satellite cloud motion at high latitudes. *Proceedings of the 8th Symposium on Meteorological Observations and Instrumentation*, Amer. Meteorol. Soc., Anaheim, CA, 17-22 January, 465-468.
- Herman, L.D. And F.W. Nagle, 1994: A comparison of POES satellite derived winds techniques in the Arctic at CIMSS. *Proceedings of the 7th Conference on Satellite Meteorology and Oceanography*, Amer. Meteorol. Soc., Monterey, CA, June 6-10, 444-447.
- Menzel, W.P., 2001: Cloud tracking with satellite imagery: From the pioneering work of Ted Fujita to the present. *Bull. Amer. Meteorol. Soc.*, 82(1), 33-47.
- Menzel, W.P. and K. Strabala, 1997: Cloud top properties and cloud phase algorithm theoretical basis document. Unpublished report, Cooperative Institute for Meteorological Satellite Studies, University of Wisconsin, 1225 W. Dayton Street, Madison, WI, 53706, 55 pp.
- Menzel, W.P., W.L. Smith, and T.R. Stewart, 1983: Improved cloud motion vector and altitude assignment using VAS. *J. Climate Appl. Meteorol.*, 22, 377-384.
- Merrill, R., 1989: Advances in the automated production of wind estimates from geostationary satellite imaging. *Proc. Fourth Conf. Satellite Meteorol.*, San Diego, CA, Amer. Meteorol. Soc., 246-249.
- Nieman, S.J., W.P. Menzel, C.M. Hayden, D. Gray, S.T. Wanzong, C.S. Velden, and J. Daniels, 1997: Fully automated cloud-drift winds in NESDIS operations. *Bull. Amer. Meteorol. Soc.*, 78(6), 1121-1133.
- Schmetz, J., K. Holmlund, J. Hoffman, B. Strauss, B. Mason, V. Gaertner, A. Koch, and L. van de Berg, 1993: Operational cloud motion winds from METEOSAT infrared images. *J. Appl. Meteorol.*, 32, 1206-1225.
- Turner, J. and D.E. Warren, 1989: Cloud track winds in the polar regions from sequences of AVHRR images. *Int. J. Remote Sensing*, 10(4), 695-703.
- Velden, C.S., C.M. Hayden, S.J. Nieman, W.P. Menzel, S. Wanzong, and J.S. Goerss, 1997: Upper-tropospheric winds derived from geostationary satellite water vapor observations. *Bull. Amer. Meteorol. Soc.*, 78(2), 173-196.
- Velden, C.S., T.L. Olander and S. Wanzong, 1998: The impact of multispectral GOES-8 wind information on Atlantic tropical cyclone track forecasts in 1995. Part 1: Dataset methodology, description and case analysis. *Mon. Wea. Rev.*, 126, 1202-1218.

MODIS Winds
6 September 2000
Band 31 (11 microns)

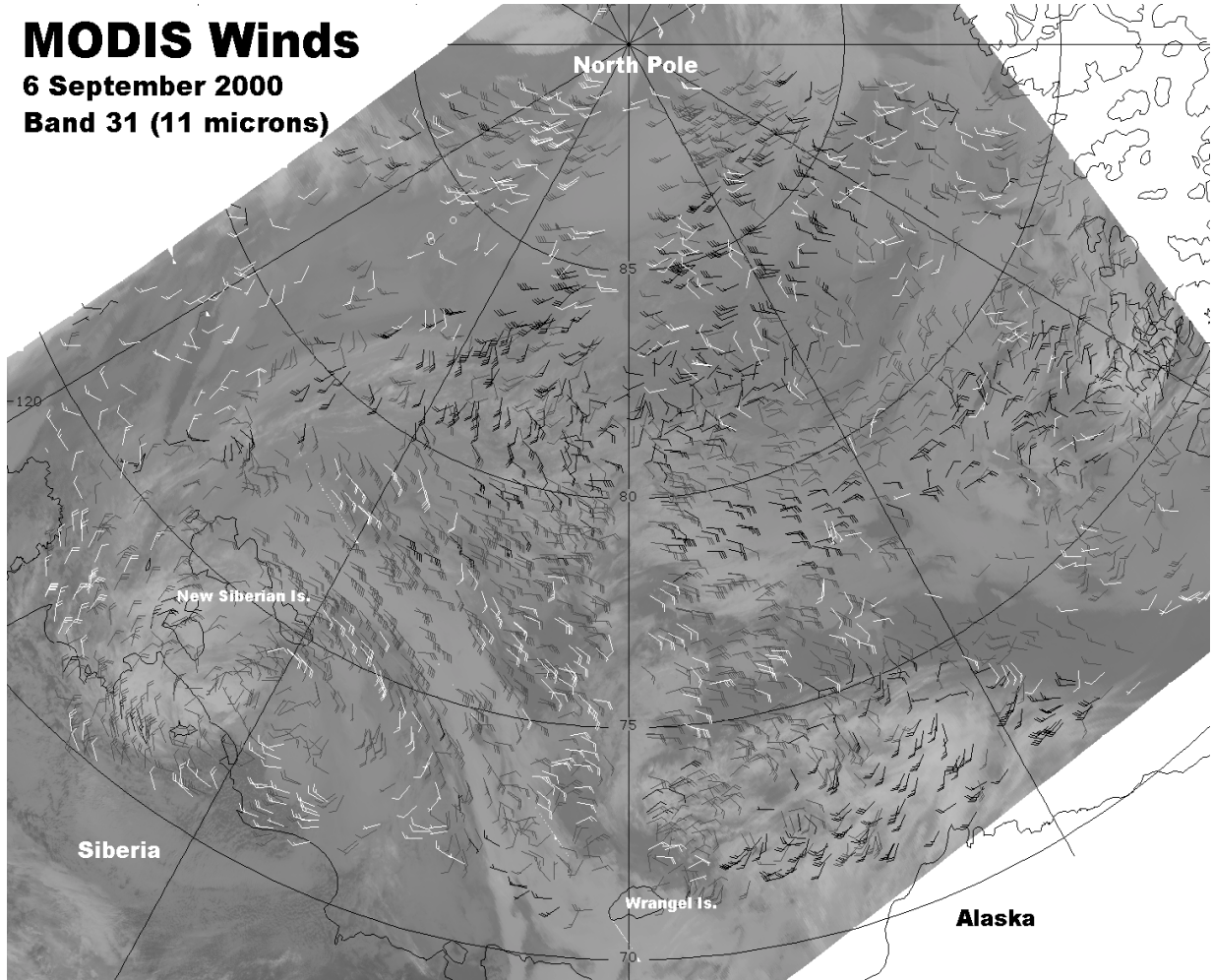


Fig. 2. Wind vectors determined with the automated cloud and water vapor tracking algorithm for 6 September 2000. Vectors are plotted on a MODIS 11 μm image, the first in the sequence of three overpasses spanning a time period of approximately 4.5 hours. Vector heights are given in three broad categories: low (white), middle (grey), and high (black).